Int. J. Heat Mass Transfer. Vol. 16, pp. 1439–1452. Pergamon Press 1973. Printed in Great Britain

MAGNETO-FLUID-MECHANIC HEAT TRANSFER FROM HOT FILM PROBES

PAUL S. LYKOUDIS and PATRICK F. DUNN

School of Aeronautics, Astronautics and Engineering Sciences, Purdue University, West Lafayette, Indiana 47907, U.S.A.

(*Received* 28 *July* 1972 *and in revised form* 17 *November* 1972)

Abstract—This paper presents results of an experimental investigation of magneto-fluid-mechanic heat transfer from quartz-coated hot film probes (0·015 cm and 0·005 cm dia) traversed vertically through a tank filled with mercury and aligned axially with a horizontal magnetic field. Findings exhibit a reduction in the probe's heat transfer due to the magnetic field in the Reynolds number range from 0 to 130 and Hartmann number range from 0 to 4·68 for magnetic interaction parameter values of order one. Four regions of heat transfer are identified, each associated with a specific flow configuration about the probe, and are described as follows:

(1) In the free convection region the magnetic field suppresses the free convective heat transfer, eventually limiting the heat transfer to thermal conduction. Heat transfer in this region is examined through an approximate solution of the momentum and energy equations.

(2) For very low Reynolds numbers of about three there is an increase in the heat transfer from the free convection state. The Reynolds number at which this initial region of forced convection becomes important is predicted by a theoretical criterion which compares free and forced convection velocities. This increase becomes detectable at a lower Reynolds number in the presence of a magnetic field.

(3) Beginning at a Reynolds number of about five, the Nusselt number can be expressed in a power law relation with the Reynolds number where the power is independent of magnetic field strength. Also a theoretical correlation is presented which determines the Reynolds numbers for various Hartmann numbers at which this stationary Föppl vortex pair initiates. The magnetic field inhibits the formation of this pattern.

(4) The generation of von Kármán vortex shedding behind the probe at a Reynolds number of about 34 yields a slight increase in the power law of the heat transfer relation which is again independent of magnetic field strength. Reynolds numbers for various Hartmann numbers at which shedding begins are represented mathematically. The magnetic field delays the onset of the vortex street and suppresses its size.

NOMENCLATURE

B,	magnetic field strength;
$C_1, \ldots, C_9$,	empirical constants;
C_p,	specific heat at constant volume;
d,	probe diameter;
Gr,	Grashof number $\equiv g\beta\Delta T d^3/\nu^2$;
g,	gravitational acceleration;
h,	film heat transfer coefficient;
k,	thermal conductivity;
l,	probe length;
M,	Hartmann number $\equiv Bd\sqrt{(\sigma/\mu)}$;
Nu,	Nusselt number $\equiv hd/K$;
Nu_c,	conduction Nusselt number;
Nu_0,	Nusselt number for zero Hartmann number;
Pr,	Prandtl number $\equiv C_p\mu/k$;
Re,	Reynolds number $\equiv dU_\infty/\nu$;
Re_0,	Reynolds number for zero Hartmann number;
Re_m,	Reynolds number for Hartmann number M;
RMS,	root-mean-square;
s,	length of Föppl vortex pair extension;
T_e,	environmental temperature;
T_p,	probe temperature;
U_∞,	probe velocity;
u,	free convection velocity;
x, y,	Cartesian coordinates;
α,	thermal diffusivity;

β, coefficient of thermal expansion;
δ, velocity boundary-layer thickness;
δ_T, thermal boundary-layer thickness;
ΔT, temperature difference $= T_p - T_e$;
λ, nondimensional parameter defined in equation (10);
μ, viscosity;
ν, kinematic viscosity;
ρ, density;
σ, electrical conductivity.

INTRODUCTION

A MAJORITY of velocity, temperature and respective fluctuating quantity measurements in Magneto-Fluid-Mechanic (MFM) flows have been obtained through use of a quartz-coated hot film probe in mercury.

Early experimentalists [1–5] using coated probes noted considerable difficulty in recording repeatable and stable heat transfer–velocity calibration curves in mercury. Calibration curve irreproducibility and lability were attributed to the variation of the thermal contact resistance layer at the probe–mercury interface essentially by the formation of an oxide impurity layer on the probe's surface. These problems necessitated the development of theories by which calibration data could be correlated with one another.

Sajben [1], using enamel-coated tungsten wires, postulated that the contaminant effect manifested itself as an additive resistance to the heat transfer from the probe. His consideration permitted this effect to be circumvented by expressing heat transfer-velocity results in the form of a new heat transfer variable. The limitations of the Sajben correction constant were in the assumptions that it was derived for an infinitely long cylinder of negligible end effects with steady state heat transfer where the Nusselt number is solely a function of the Péclét number. Sajben noted that $Nu(0)$ (present in the expression of the Sajben correction constant) should be interpreted as a reference value other than at Péclét number equal to zero, where the Nusselt number may be a function of the Grashof and Hartmann numbers. Sajben demonstrated that when this procedure was correctly applied various heat transfer–velocity data could be correlated exceptionally well within the range $0 \leqslant Pe' \leqslant 1$. Zero flow referencing by Malcolm [7] resulted in a divergence of his data as the Péclét number approached a value of one.

Hua [3] also incorporated the concept of an impurity coating in his development of a semi-empirical theory for the heat transfer from quartz-coated probes in mercury. He proposed that the flow about the probe be divided into a stationary fluid inner region and an inviscid flow outer region. By properly choosing the dimensions of an ellipsoidal-shaped displacement boundary Hua was able to match his and Sajben's calibration data with theoretically predicted values. In Hua's theory the displacement boundary shape and impurity constant were determined experimentally.

Hoff [8] surmounted the quartz–mercury interface problem by depositing a fine layer of gold or copper on the probe's quartz surface. Using this approach he found excellent agreement with the theory of Grosh and Cess [9] for heat transfer from cylinders to fluid of low Prandtl numbers.

In a review of hot film anemometry in mercury Gardner* [10] demonstrated that, when the effect of an impurity fouling factor was accounted for, the data of Hua [3], Hoff [8] and Hill [12] agreed with both the theory of Gross and Cess [9] and Hua [3] for $1 \leqslant Pe' \leqslant 15$. In the range $0 \leqslant Pe' \leqslant 1$ the theory of Gross and Cess underestimated the experimental data. Throughout the entire Péclét number range the data of Hua upon consideration of the impurity constant was found to be within 1 per cent of values predicted by King's Law [13]. Gardner concluded that it was possible to correlate hot film

* Also refer to Hill and Sleicher [11] for an extensive review of heat transfer from finite and infinite length cylinders.

probe calibration data in mercury with existing semi-empirical laws when including the impurity factor.

Magneto-Fluid-Mechanic effects on the heat transfer from the hot film probe were also considered. Magnetic field dampening of free convective heat transfer was qualitatively observed and first reported by Gardner [14].

Malcolm [15] presented a calibration curve correction procedure for the case of parallel probe axis orientation with the magnetic field for strengths greater than 4000 Gauss. This procedure was based on free convection measurements for one Grashof number case and the assumption that MFM effects on forced convection were absent for the specified geometry. It will be seen later that our experimental results refute Malcolm's assertions.

Recently Platnieks [16], using tungsten wire probes in mercury insulated by a fine layer of silicon monoxide, reported no measureable MFM reduction of the probe's heat transfer over the forced convection range $8 \leqslant Re \leqslant 48$. These experiments were performed at low magnetic interaction values (of the order 10^{-3} or less).*

EXPERIMENTAL APPARATUS

In the present investigation quartz-coated hot film probes were calibrated in a tank filled with mercury with and without the application of a horizontal magnetic field aligned parallel with the probe's axis (Fig. 1(a)). These calibrations were accomplished by traversing a Thermo-Systems Inc. 1210–60 Hg ($l = 0{\cdot}200$ cm and $d = 0{\cdot}015$ cm) or 1210–20 Hg ($l = 0{\cdot}100$ cm and $d = 0{\cdot}005$ cm) quartz-coated platinum hot film probe† vertically at various constant velocities through a tank filled with mercury and recording its bridge voltage output. The calibrating system

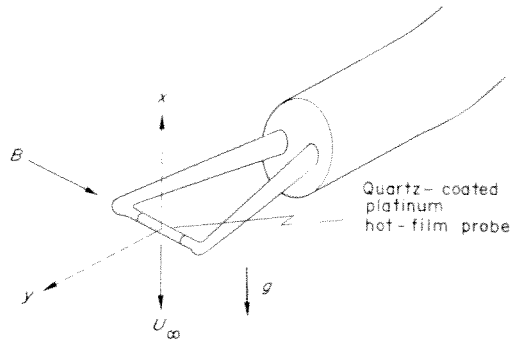

FIG. 1(a). The geometry of the problem.

was designed to be minimally free of vibrations over a range of constant velocities (0–10 cm/s).

The calibrating mechanism was housed in an iron structure mounted atop the Purdue University Magneto-Fluid-Mechanic Laboratory's electromagnet (Fig. 1(b)). A stainless steel bar, into which the probe holder was press-fitted, was connected to the front of a support plate. This plate was traversed by means of a vertical turn screw positioned through its center. The turn screw was driven via a Pic belt and pulleys by a variable speed motor. A linear bearing-guide rod system was aligned parallel to the turn screw and passed through the support plate to assure smooth travel.

The probe holder extended down into a rectangular stainless steel tank (15·2 cm × 5·7 cm × 73·7 cm) placed between the pole-faces of the electromagnet. The tank was filled with triple-distilled mercury (~ 6200 cm^3).

The water cooled d.c. electromagnet was powered by a d.c. motor-generator set. A maximum field of 15 000 Gauss could be obtained in the electromagnet's gap (7·7 cm) between its polefaces (30·5 cm × 147·0 cm).

MEASUREMENTS

The essential parameters measured were the probe velocity, the environmental temperature of mercury, the average bridge voltage of the anemometry system and the magnetic field strength.

* The *maximum* value of the interaction parameter was found to be 0·005 based on a Reynolds number of 10 and a magnetic field strength of 8000 Gauss where the characteristic length was chosen to be the diameter of the probe.

† Platinum films were used to avoid magnetic effects observed with films of magneto-resistive materials, e.g. nickel [16].

The test region was located from 3 cm after the beginning to 3 cm before the end of the pole-face region. Two microswitches were positioned on the traversing mechanism structure. As the probe travelled through the test region, each microswitch was triggered at the appropriate time, sending start and stop commands to the various recording equipment.

The velocity was computed from the distance between the microswitches (25·4 cm) and the time recorded on a Universal time counter. A linear potentiometer was mounted on the top of the structure to check for constant velocity. A string was wound around its axis and connected to the probe support plate. The output of the potentiometer, connected in series with a 15-V dry cell, was displayed on a Tektronix storage oscilloscope. A linear trace indicated a constant velocity.

The environmental temperature of the mercury was measured from an iron–constantan thermocouple placed in the center of the test region; experimental measurements verified the same temperature throughout the mercury environment. It was monitored on a VIDAR integrating digital voltmeter.

An integrated bridge voltage from the output of a Thermo-Systems Inc. 1050 constant temperature anemometer was obtained by using the microswitches. From this integrated bridge voltage and the time of traverse, an average bridge voltage was calculated. The anemometer output was also connected to a Thermo-Systems Inc. RMS voltmeter to check if vibrations in the system produced significant velocity fluctuations ($>0{\cdot}5$ per cent RMS).

The magnetic field strength was measured from the voltage drop of a shunt in series with the coil of the electromagnet (calibrated with a Scalamp fluxmeter).

The experimental scheme included the measurement of a stable and repeatable calibration curve for the non-magnetic case. This usually was not accomplished before approximately 50 probe operating hours in the same mercury environment. During this initial period Nusselt number values were found to differ by as much as 10 per cent for the same Reynolds number. Eventually these variations subsided and Nusselt numbers could be repeatedly measured within 1·1 per cent error. This anomalous behavior can possibly be attributed to a wetting of or impurity deposition upon the probe–mercury interface which developed over a period of time and finally established a uniform rate of heat transfer between the probe and the environment.

Once repeatability was established, a calibration within a magnetic field was determined. This was followed by a verification that the non-magnetic case curve had not altered during measurements within a magnetic field. This procedure was repeated after all magnetic cases examined. Each experimental trial at a velocity was executed three times to further insure reproducibility of the data.

Calibrations throughout the entire Reynolds and Hartmann number range investigated were obtained for two different 0·015 cm dia probes operated at approximately the same temperature difference with the environment ($\Delta T \sim 46^{\circ}C$). Additional measurements at zero Reynolds number were made using 0·015 cm and 0·005 cm diameter probes each operated at two temperature differences ($\Delta T \sim 21^{\circ}C$ and $\sim 43^{\circ}C$). Initial observations at zero Reynolds number indicated a variation of heat transfer values about some mean (which has been previously observed [17]). Therefore, the time period over which the measurements were integrated was increased (to over 300 s) until repeatability of the same heat transfer data was attained (within 1·1 per cent error).

Additional errors associated with instrumentation involved in measurements of the Nusselt, Reynolds and Hartmann numbers were found to be 0·07, 0·88 and 0·50 per cent respectively.

RESULTS

The heat transfer from the probe was correlated with the velocity and magnetic field

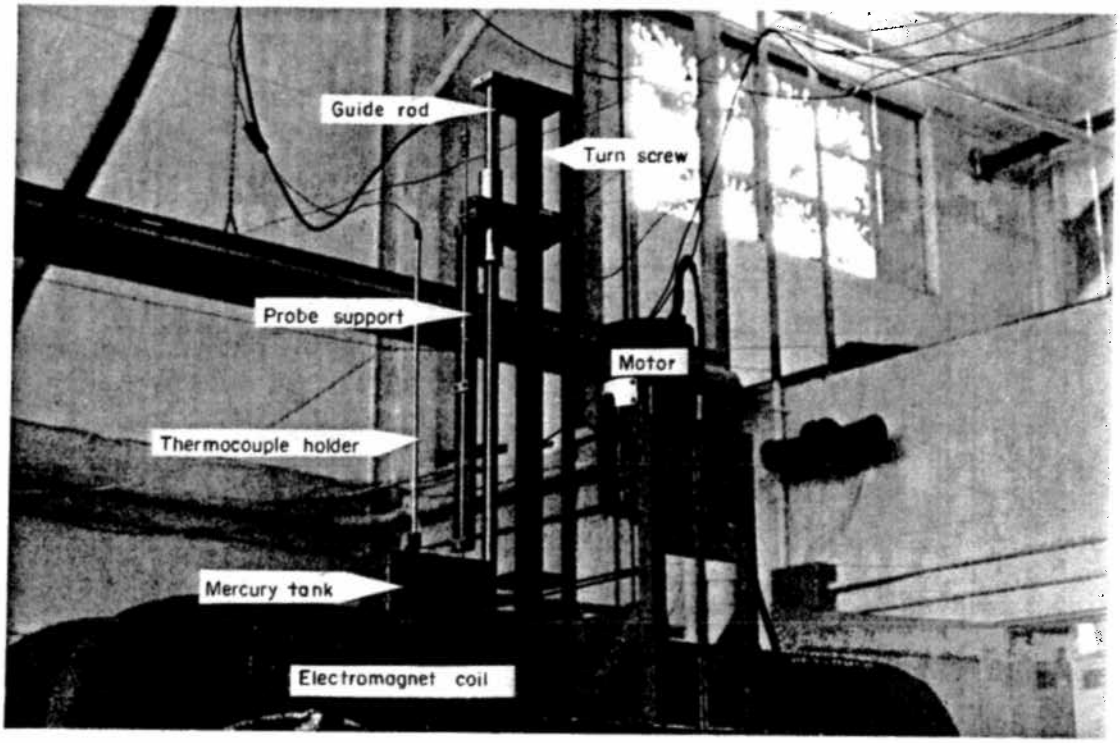

FIG. 1(b). The experimental apparatus.

strength through the non-dimensional Nusselt, Reynolds and Hartmann numbers.

The expression for the Nusselt number was found by equating the power supplied to the probe with the heat flux from the probe to the mercury. All Nusselt numbers were referred to the same temperature [18]. The characteristic length in the Reynolds and Hartmann numbers was chosen to be the diameter of the probe. The respective Reynolds and Hartmann numbers for each Nusselt number were calculated.

Calibration curves of the Nusselt number versus the Reynolds number for zero Hartmann number exhibited the same characteristics of curves obtained by previous experimentalists using hot film probes in mercury. These zero Hartmann number data when expressed in the form of the Sajben correction constant versus Péclét number were found to agree well with the data of Hill and Sleicher [6] and of Malcolm [7] when using their zero referencing procedure.

Nondimensional results were plotted as the logarithm of the Nusselt number versus the logarithm of the Reynolds number to examine if any power relations existed (Fig. 2). Four distinct regions of heat transfer were identified.

Region A was characterized by constant Nusselt number lines which extended from zero Reynolds number up to a critical Reynolds number. This critical Reynolds number, which decreased for increasing Hartmann numbers, is indicated in Fig. 2 by dotted line 1.

Region B was marked by increasing Nusselt number values for increasing Reynolds numbers. This region extended over a wider Reynolds number range in the magnetic case. Its termination occurred along a constant Nusselt number line shown in Fig. 2 by dotted line 2.

In *Region C* the Nusselt number was directly proportional to the Reynolds number raised to the 0·24 power. Although the onset of this region was delayed in the presence of a magnetic field, the power relation remained the same. Region C ended along a constant Nusselt number line shown as in Fig. 2 by dotted line 3.

Region D exhibited a trend similar to Region C but was marked by an increase in the power of the Reynolds number in the heat transfer relation from 0·24 to 0·27.

It is noted that power laws found in Regions

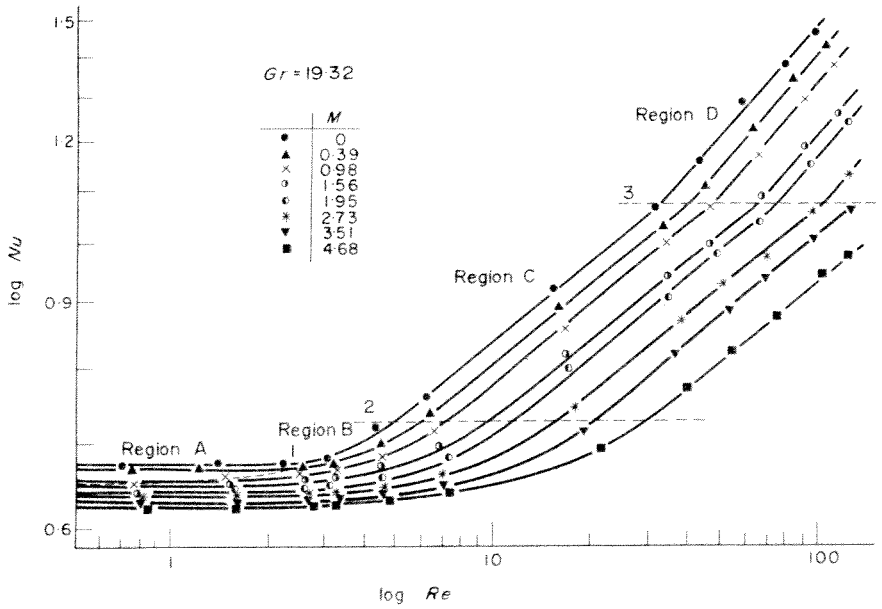

FIG. 2. Nondimensional calibration curves at different Hartmann numbers.

C and D varied for each hot film probe. Power laws found in Region C varied between 0·12 and 0·26 and in Region D between 0·25 and 0·50. These power law variations within a region for different probes (also exhibited in the calibrations of other investigators calibrating in mercury [3, 11]) were attributed to the fouling effects which physically alter the magnitude of the heat transferred from the probe. However, the aforementioned experimental procedure assures that these effects remained constant throughout the experiment. Nusselt number results presented in this paper therefore include the inherent effects of fouling on the probe's heat transfer.

THEORETICAL CONSIDERATIONS

The current experimental results infer that magnetic field effects are exhibited through the inhibition of the convective mechanisms of heat transfer. The four regions of heat transfer were postulated to correspond to the following fluid mechanical convective mechanisms: free convection, initial forced convection, the formation and growth of the stationary Föppl vortex pair and von Kármán vortex shedding (Fig. 3) [19].

(A) *The region of free convection.* The exact solution of heat transfer from a finite probe* entails the consideration of three-dimensional variations in velocity and temperature accompanied by heat conduction loss to the supports. A simplification is made by acknowledging that a majority of the heat transferred from the probe can be expressed in the case of two-dimensional free convection.

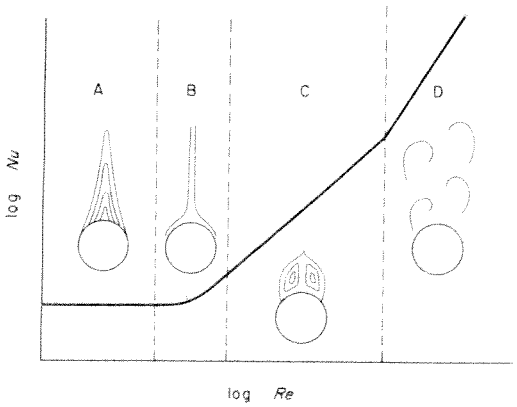

FIG. 3. A qualitative calibration curve with postulated flow configurations.

When examining free convection from a small diameter cylinder the velocity is so small that the inertia term involving the square of the velocity can be neglected. Further, the viscous dissipation term is negligible. Because there is no external pressure gradient imposed on the flow, the pressure force in the vertical direction becomes zero. Thus, the conservation equations of momentum in the x-direction (Fig. 1) and energy can be written as:

$$0 = \mu \frac{\partial^2 u}{\partial y^2} - \sigma B^2 u + g\beta\rho\Delta T \qquad (1)$$

and

$$u \frac{\partial T}{\partial x} = \alpha \frac{\partial^2 T}{\partial y^2}. \qquad (2)$$

The ponderomotive force $(-\sigma B^2 u)$ and the bouyancy force $(g\beta\rho\Delta T)$ represent the body forces per unit volume, where ΔT is the temperature difference between the probe's platinum film and the environment.

The mathematical difficulty encountered in obtaining an exact solution of the free convection equations for small diameter cylinders lead us to consider an approximate method by which essential results could still be found. Here, an order of magnitude analysis of the type offered by Lykoudis and Yu [20] was employed. The order of magnitude equations corresponding to equation (1) and equation (2) can be written as:

$$0 = -\mu \frac{u}{\delta^2} - C_1 \sigma B^2 u + C_2 g\beta\rho\Delta T \qquad (3)$$

and

$$C_3 u \frac{\Delta T}{d} = \alpha \frac{\Delta T}{\delta T^2}. \qquad (4)$$

The constants C_1, C_2 and C_3 are empirical.

* $l/d = 13{\cdot}3$ for the 0·015 cm dia probe and $l/d = 20{\cdot}0$ for the 0·005 cm dia probe.

This analysis permits the necessary uncoupling of the momentum and energy equations by substituting into equation (3) the expression for the free convection velocity, u, found from equation (4). The resulting equation can be nondimensionalized and solved for the Nusselt number by employing the equation:

$$Nu = \frac{hd}{K} \sim \frac{d}{\delta_T} \sim \frac{d}{\delta}\sqrt{(Pr)}. \tag{5}$$

One obtains:*

$$Nu = \sqrt{\left(\frac{2GrPr/C_4}{M^2 + \sqrt{(M^4 + 4GrC_5/C_4^2)}}\right)} \tag{6}$$

where

$$C_4 = \frac{C_1}{C_2C_3} \text{ and } C_5 = \frac{1}{C_2C_3}. \tag{7}$$

This expression for the free convection above a horizontal cylinder in a magnetic field differs only in the constants from the momentum integral solution by Lykoudis [21] for the natural convection from a vertical hot plate in the presence of a magnetic field.

It was observed experimentally that as M became large the Nusselt number approached a limiting value (the conduction Nusselt number, Nu_c). Equation (6), then, is amended to read as:

$$Nu = Nu_c + \sqrt{\left(\frac{2GrPr/C_4}{M^2 + \sqrt{(M^4 + 4GrC_5/C_4^2)}}\right)}. \tag{8}$$

For the zero Hartmann number case this expression reduces to:

$$Nu_0 = Nu_c + \left(\frac{Gr}{C_5}\right)^{\frac{1}{4}}\sqrt{(Pr)}. \tag{9}$$

Equations (8) and (9) can be combined to form the nondimensional parameter λ:

$$\lambda = \frac{Nu - Nu_c}{Nu_0 - Nu_c} = \sqrt{\left(\frac{\sqrt{(C_6Gr)}}{M^2 + \sqrt{(M^4 + C_6Gr)}}\right)} \tag{10}$$

where

$$C_6 = 4C_5/C_4^2. \tag{11}$$

Here λ expresses the ratio of free convective heat transfer present within a magnetic field to the total free convective heat transfer in the non-magnetic case. C_6 is the only constant which need be determined experimentally. In Fig. 4(a) equation (10) is compared with the experimental results obtained operating a 0·015 cm dia probe for two separate Grashof number cases ($\Delta T = 46{\cdot}3$°C and 23·7°C). It is noted that C_6, determined from one experimental measurement, remained constant in both

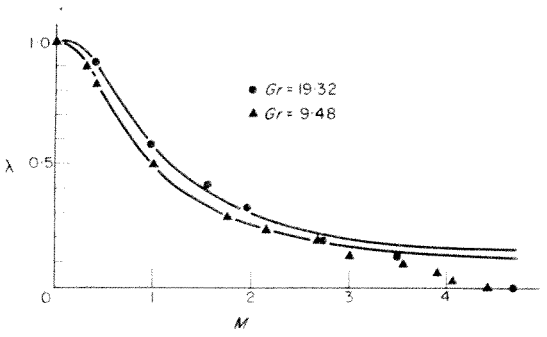

FIG. 4(a). Parameter λ at different Hartmann numbers for 0·015 cm dia probe.

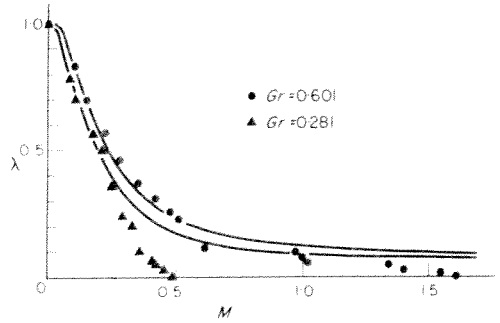

FIG. 4(b). Parameter λ at different Hartmann numbers for 0·005 cm dia probe.

* The positive sign of the square root term in the denominator of equation (6) is taken since Nu was observed to decrease with increasing M.

cases ($C_6 = 0{\cdot}0296$). It is seen that as λ becomes small, there is a deviation of the experimental values from the predicted results. This occurs when conduction becomes the predominant mechanism of heat transfer and equation (10) can no longer be interpreted as a valid expression for the heat transfer process.

In order to examine the consequences of a wider variation in the Grashof number and to ascertain the possible universality of C_6 for all probes we obtained experimental results (Fig. 4(b)) by operating a 0·005 cm dia probe for two additional Grashof number cases ($\Delta T = 40{\cdot}6^\circ$C and 19·0°C). In these cases the value of C_6 was determined to be 0·0015. This variation among probes can be understood phenomenologically by the presence of an impurity coating on the probe's surface whose inhibitive effect on the heat transfer is greater for larger diameter probes.

These results yield that the magnetic field strength needed for complete suppression of free convection varies with Grashof number. This effect was not considered in the free convection correction procedure of Malcolm [15].

(B) *The region of initial forced convection.* If we examine an expanded representation of the heat transfer data for low Reynolds numbers as shown in Fig. 5 we observe that the departure from the constant free convection Nusselt number line occurs at a Reynolds number of about three for the non magnetic case. Further, for increasing Hartmann numbers this rise in heat transfer occurs at lower Reynolds numbers.

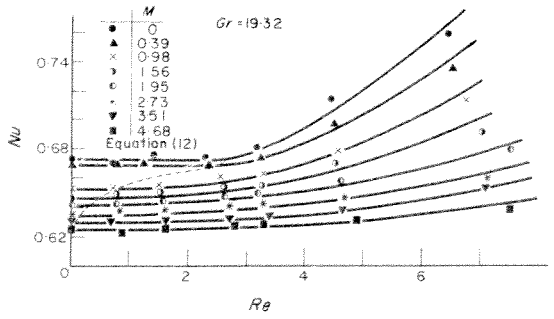

FIG. 5. Nondimensional calibration curves at different Hartmann numbers for low Reynolds numbers.

This increase in the Nusselt number for increasing Reynolds number is indicative of a new heat transfer mechanism. This region begins when the forced convection velocity exceeds the free convection velocity. This statement can be phrased in an inequality. We note that the order of magnitude of the free convection velocity is given by equation (4). After the usual nondimensionalization to introduce the appropriate nondimensional numbers, this inequality is expressed as:

$$Re > \frac{1}{C_3}\left[\frac{2Gr/C_4}{M^2 + \sqrt{(M^4 + C_6 Gr)}}\right]. \quad (12)$$

Since the coefficient C_6 was determined before in the case of free convection, only one heat transfer measurement within a magnetic field is required to fix the coefficient product $1/C_3C_4$, thereby completely defining inequality (12). Inequality (12) is compared with experiments at various Hartmann numbers in Fig. 5. The deviation from experimental results at large Hartmann numbers is expected since inequality (12) will not be valid when conduction is prominent.

Inequality (12) can be further employed to examine the zero Hartmann number case. It reduces to:

$$Re_0 > C_7\sqrt{(Gr)} \quad (13)$$

where

$$C_7 = \sqrt{(C_2/C_3)}. \quad (14)$$

This square root criterion simply implies that the inertia force must exceed the buoyancy force for a rise in heat transfer to occur.

When we first encountered this result which so completely describes the heat transfer rise throughout the Hartmann number cases examined, we found an apparent variance with the classical cubic root approximating criterion established by Collis and Williams [22]. They advanced that the Reynolds number must exceed tbe cubic root of the Grashof number in order for forced convection to begin. This situation

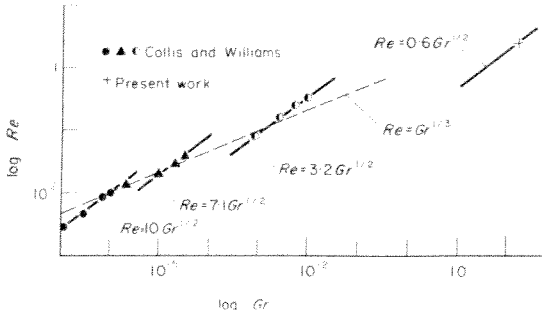

FIG. 6. Comparison with experiment of criterion for the onset of forced convection.

prompted a reexamination of their data from heated horizontal wires in air (Fig. 6). The discrepancy was resolved when we observed in the light of the current finding that the square root criterion or inequality (13) actually agreed more exactly with their data than their cubic root criterion. Here C_7 was determined for each case.

We concluded that in order to exactly determine the Reynolds number at which forced convection begins for a particular Grashof number case one must employ the analysis presented above and determine experimentally the coefficient C_7. However, the cubic root criterion remains a more convenient approximating criterion in that an experimental coefficient need not be determined. Values within an error of less than 30 per cent of those measured can be obtained using this approximation (see Fig. 6).

An analysis describing MFM heat transfer throughout the initial region of forced convection was not attempted since the underlying convection mechanism is not well understood.

(C) *The region of the stationary Föppl vortex pair.* Let us now draw a constant Nusselt number line passing through the point of the zero magnetic field line in Fig. 2 where the Reynolds number is equal to five. We see that the intersection of this line with all other heat transfer lines for different magnetic fields is along a line above which the Nusselt number dependence on the Reynolds number is given by a power law. Furthermore, we observe that this power law is the same, regardless of the intensity of the magnetic field. Because of this behavior, we postulate that regardless of the intensity of the magnetic field, as soon as the stationary Föppl vortices have been formed, the heat transfer rates will be the same.

We now wish to predict theoretically the Reynolds number at which the Föppl vortices are formed, that is the Reynolds numbers corresponding to the intersection of the line separating Region B to C for different magnetic fields. In order to answer this question, we sought guidance through the work of Chester [23], Payne and Pell [24], and Chang [25] who have computed drag coefficients at low Reynolds numbers for various axially symmetric bodies in the presence of aligned magnetic fields. Their results are typically presented in the following form:

$$\frac{(\text{Drag})_m}{(\text{Drag})_0} = 1 + C_8 M + C_9 M^2. \qquad (15)$$

Since for small Reynolds numbers the drag is proportional to the velocity, one could use the above correlation as an indication of the ratio of the two critical Reynolds numbers at which the Föppl stationary vortices are formed. Furthermore, since we can use at least two of our experimental results from Fig. 2 to determine the two coefficients C_8 and C_9, we could check the validity of this representation. In fact, a least square best fit of all of the data was used and the result is the following:

$$\frac{Re_m}{Re_0} = 1 + 0{\cdot}355\,M + 0{\cdot}155\,M^2. \qquad (16)$$

Figure 7 compares this equation with all of our data and it seems that the fit is fairly good. The value of the coefficient C_8 in the above equation is very close to the ones theoretically computed by Chang [25], Chester [23] notwithstanding the fact that their work refers to Reynolds numbers lower than five. Example values of C_8 are 0·318 for a flat disc and 0·375 for a sphere. On the other hand, their values of C_9 are of

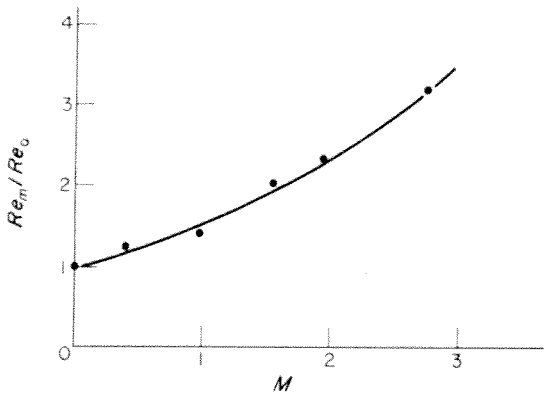

FIG. 7. Föppl vortex pool formation at different Hartmann numbers.

order zero, which differ from the value found in our case. The result of the above equation implies that in the presence of the magnetic field, the probe must be traversed at a higher Reynolds number in order to obtain the same heat transfer value as in the non magnetic case.

(D) *The von Kármán vortex region.* The observed change in the convective heat transfer mechanism, described by an increase in the power of the Reynolds number for the Nusselt number–Reynolds number relation (Fig. 2), marks the initiation of shedding of the stationary vortex pattern from behind the probe.

Experimental results for the zero Hartmann number case establish the onset of vortex shedding at a Reynolds number of about 40 [26]. In the present investigation a change in the heat transfer process occurred at a Reynolds number of 34. This somewhat premature manifestation could be attributed to small vibrations of the moving probe which lowered the initial shedding frequency [26].

Magneto-fluid-mechanic vortex shedding from a cylinder in a crossflow of mercury has been examined by Papailiou [27]. He experimentally observed by traversing various diameter cylinders through a tray filled with mercury that the application of a magnetic field parallel to the axis of the cylinder (for $0{\cdot}02 \leqslant M^2/Re \leqslant 6$) suppressed the size of the von Kármán vortex street.

We shall now attempt to determine the locus of transition from Region C to Region D. Here again, we observe that if we trace a constant Nusselt line passing from the intersection of the zero magnetic field line of Fig. 2 at Reynolds number 34 (the point after which in our experiments von Kármán shedding has started), we find that this line intersects other lines at a point where transition from one power law to another occurs. For this reason, we postulate that shedding will occur in the presence of the magnetic field when the stationary vortices reach the same size at which they would have separated in the ordinary fluid mechanical case. It is well known that Taneda [28] has shown that the length of this quasi-stagnant region behind a cylinder grows linearly with increasing Reynolds numbers (see Fig. 8). Its

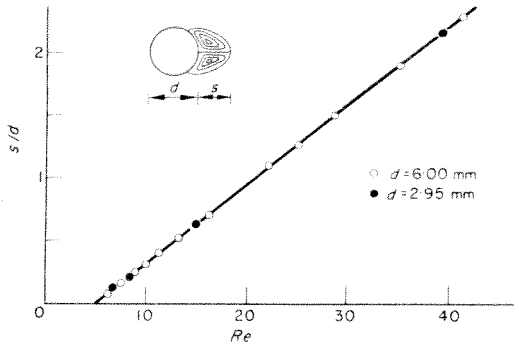

FIG. 8. Taneda's [28] experimental results.

limit is, of course, at a Reynolds number around 40 where wake instabilities produce detachment from the cylinder. The theoretical determination of the critical Reynolds number after which the Föppl vortices will become free von Kármán vortices is a difficult task. In order, however, to answer this question, we felt that an equation similar to equation (15) might be appropriate. Application of this formula in this case by use of our experimental results has given us the

same equation which is tested in Fig. 9 where the dots represent our experimental data.

As in Region C the power in the Nusselt number–Reynolds number relationship remained constant for varied magnetic fields.

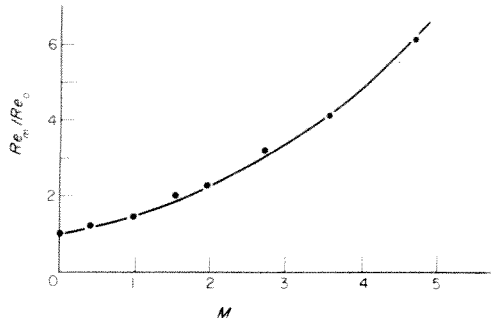

FIG. 9. von Kármán vortex shedding at different Hartmann numbers.

Further, only a slight variation in h from Region C to Region D was observed (also exhibited in the data of Hill and Sleicher [6]). This minimal effect of the additional convective mechanism upon the probe's heat transfer is the result of the high thermal conductivity of mercury.

The observed MFM reduction of forced convective heat transfer demonstrates that magnetic field interaction is present for magnetic interaction parameter values above approximately 0·02. An order of magnitude argument supports that MFM effects should be present for values of order one. Here, the ponderomotive force is on the order of the inertia force. Further, Platnieks' experiment shows that when magnetic interaction parameter values become lower MFM effects upon the probe's heat transfer are not measureable.

As stated earlier, these forced convection results are in variance with Malcolm's findings. Malcolm [15] states that in the case when the magnetic field is aligned parallel to the probe axis and perpendicular to the forced convection flow we would expect no interaction of the magnetic field with the flow. His argument is based upon a theorem stated in Shercliff's book [29], namely that in a two-dimensional magneto-fluid-mechanic flow wherever the flow's vorticity vector is aligned parallel to the magnetic field there will be no MFM interaction with the flow. This theorem is correct except that although the two-dimensionality of the fluid flow and the magnetic field can be maintained, the current lines that can be induced certainly will do so in a three-dimensional fashion, thus annulling the premises on which the theorem rests. In addition, Malcolm did not support his assertions by making measurements in the forced convection region [30]. In fact, our findings show that considerable interaction of the magnetic field with the flow exists.

CONCLUSIONS

The primary result of the present work is the experimental discovery of four characteristic regions of MFM heat transfer from a hot film probe in the Reynolds number range from 0 to 130. Heat transfer in these four regions is damped by a magnetic field at which the ponderomotive over inertia forces are of order one. These findings are supported through approximate solutions of the governing conservation equations. A summary of each region follows.

(A) *The region of free convection.* The effect of the magnetic field was to suppress the free convection, allowing conduction to become the major heat transfer mechanism at higher Hartmann numbers. The heat transfer of the probe for various Hartmann number cases at zero Reynolds number was described by an order of magnitude approximation of the momentum and energy equations.

(B) *The region of initial forced convection.* The presence of the magnetic field lowered the Reynolds number at which the onset of forced convection occurred. The onset of this region mathematically was represented by an expression which compares free and forced convection velocities. This criterion predicted the beginning of forced convection except for high Hartmann numbers.

(C) *The region of the stationary Föppl vortex pair.* The magnetic field acted to delay the Föppl vortex pair formation. A theoretical correlation of the Reynolds numbers as a function of Hartmann numbers at which transition occurs from Regions B to C is offered. The power in the Nusselt number–Reynolds number relation was found to be independent of magnetic field strength.

(D) *The von Kármán vortex region.* The magnetic field acted to suppress the size of the von Kármán vortex street. A theoretical correlation of the Reynolds numbers as a function of Hartmann numbers at which transition occurs from Regions C to D is presented. Vortex shedding slightly increased the power in the heat transfer relation which was found to be independent of magnetic field strength.

The analysis presented above provides a description of MFM heat transfer from hot film probes for $0 \leqslant Re \leqslant 130$ and $0 \leqslant M \leqslant 4{\cdot}68$ where M^2/Re is of order one. Specific quantitative relations for each probe can be found for all Hartmann numbers.

ACKNOWLEDGEMENTS

The authors wish to acknowledge the persons of the MFM group at Purdue University for their many helpful discussions. Also, the financial assistance of the National Science Foundation under Grant GK-23694 is gratefully appreciated.

REFERENCES

1. M. Sajben, Hot wire measurements in a liquid mercury jet subject to a magnetic field, Sc.D. Thesis, Massachusetts Institute of Technology, Cambridge (1964).
2. D. G. Malcolm, Some aspects of turbulence measurements in liquid mercury using cylindrical quartz-insulated hot-film sensors, University of Warwick, Coventry (1968).
3. H. M. Hua, Heat transfer from a constant temperature circular cylinder in cross-flow and turbulence measurements in a MFM channel, Ph.D. Thesis, Purdue University, Lafayette (1968).
4. D. C. Easley, Characteristics of a hot film anemometer in a liquid mercury system, M.S. Thesis, Purdue University, Lafayette (1966).
5. M. Sajben, Hot wire anemometer in liquid mercury, *Rev. Scient. Instrum.* **36**, 945–949 (1965).
6. J. C. Hill and C. A. Sleicher, Directional sensitivity of hot film sensors in liquid metals, *Rev. Scient. Instrum.* **42**, 1461–1468 (1971).
7. D. G. Malcolm, Some aspects of turbulence measurement in liquid mercury using cylindrical quartz-insulated hot-film sensors, *J. Fluid Mech.* **37**, 701–714 (1969).
8. M. Hoff, Hot-film anemometry in liquid mercury, *Instrum. Control Syst.* **42**, 83–86 (1969).
9. R. J. Grosh and R. D. Cess, Heat transfer to fluids with low Prandtl numbers for flow across plates and cylinders of various cross section, *Trans. Am. Soc. Mech. Engrs* **80**, 667–676 (1958).
10. R. A. Gardner, Hot film anemometry in a liquid mercury magneto-fluid-mechanic pipe flow, Paper No. 2-2-55, Symposium on flow, its measurement and control in science and industry, Pittsburgh (1971).
11. J. C. Hill and C. A. Sleicher, Convective heat transfer from small cylinders to mercury, *Int. J. Heat Mass Transfer* **12**, 1595–1604 (1969).
12. J. C. Hill, The directional sensitivity of a hot-film anemometer in mercury, Ph.D. Thesis, University of Washington, Seattle (1968).
13. L. V. King, On the convection of heat from small cylinders in a stream of fluid: determination of the convection constants of small platinum wires with applications to hot-wire anemometry, *Phil. Trans. R. Soc.* **214A**, 373–432 (1914).
14. R. A. Gardner, Magneto-fluid-mechanic pipe flow in a transverse magnetic field with and without heat transfer, Ph.D. Thesis, Purdue University, Lafayette (1969).
15. D. G. Malcom, Magnetohydrodynamic effects on hot-film measurements in mercury, *DISA Inform. Bull.* **9**, 27–29 (1970).
16. I. A. Platnieks, Comparison of the hot wire anemometer and conduction methods for mercury measurements, *Magn. Gidrodin.* **7**(3), 140–142 (1971).
17. R. A. Gardner, Washington University, Personal Communication (1971).
18. Thermo-Systems Inc., Hot film and hot wire anemometry, Theory and Applic. Bull. TB5.
19. P. F. Dunn, Magneto-fluid-mechanic natural and forced heat transfer from horizontal hot film probes, M.S. Thesis, Purdue University, Lafayette (1971).
20. P. S. Lykoudis and C. P. Yu, The influence of electrostrictive forces in natural thermal convection, *Int. J. Heat Mass Transfer* **6**, 853–862 (1963).
21. P. S. Lykoudis, Natural convection of an electrically conducting fluid in the presence of a magnetic field, *Int. J. Heat Mass Transfer* **5**, 23–34 (1962).
22. D. C. Collis and M. J. Williams, Two-dimensional convection from heated wires at low Reynolds numbers, *J. Fluid Mech.* **6**, 357–384 (1959).
23. W. Chester, The effect of a magnetic field on Stokes flow in a conducting fluid, *J. Fluid Mech.* **3**, 304–308 (1958).
24. L. E. Payne and W. H. Pell, The Stokes flow problem for a class of axially symmetric bodies, *J. Fluid Mech.* **7**, 529–549 (1960).
25. I-Dee Chang, Stokes flow of a conducting fluid past an axially symmetric body in the presence of a uniform magnetic field, *J. Fluid Mech.* **9**, 473–477 (1960).

26. A. W. MARRIS, A review on vortex streets, periodic wakes, and induced vibration phenomena, *Trans. Am. Soc. Mech. Engrs* **86**, 185–196 (1964).
27. D. D. PAPAILIOU, Magneto-fluid-mechanic vortex street (part II), Ph.D. Thesis, Purdue University, Lafayette (1971).
28. S. TANEDA, Experimental investigation of the wakes behind cylinders and plates at low Reynolds numbers, *J. Phys. Soc. Japan* **11**, 302–307 (1956).
29. J. A. SHERCLIFF, *A Textbook of Magnetohydrodynamics*, pp. 86–87. Pergamon Press, Oxford (1965).
30. D. G. MALCOLM, University of Saskatchewan, Personal Communication (1972).

TRANSFERT THERMIQUE A PARTIR DE SONDES A FILM CHAUD EN MHD

Résumé—Cet article présente une recherche expérimentale de transfert thermique en MHD depuis des sondes de quartz recouvertes d'un film chaud (0,015 cm et 0,005 cm de diamètre) traversées verticalement dans un réservoir rempli de mercure et alignées axialement avec un champ magnétique horizontal. Les résultats montrent dans la sonde une réduction du transfert thermique due au champ magnétique dans les domaines du nombre de Reynolds de 0 à 130 et du nombre de Hartmann de 0 à 4.68 pour des valeurs du paramètre d'interaction magnétique de l'ordre de l'unité. On a identifié quatre régions de transfert thermique chacune d'elle étant associée à une configuration d'écoulement spécifique au voisinage de la sonde et on les décrit ainsi:

(1) Dans la région de convection libre, le champ magnétique supprime le transfert thermique par convection libre, limitant éventuellement le transfert thermique à la conduction thermique. Le transfert thermique dans cette région est examiné au travers d'une solution approchée des équations de quantité de mouvement et d'énergie.

(2) Pour des très faibles nombres de Reynolds d'environ trois, il se produit une augmentation dans le transfert thermique depuis l'état de convection libre. Le nombre de Reynolds pour lequel cette région initiale de convection forcée devient importante est estimé par un critère théorique qui compare les vitesses de convections libre et forcée. Cette augmentation devient détectable pour un faible nombre de Reynolds en présence d'un champ magnétique.

(3) A partir d'un nombre de Reynolds d'environ cinq, le nombre de Nusselt peut être exprimé par une formule en loi de puissance du nombre de Reynolds où la puissance est indépendante de l'intensité du champ magnétique. On présente aussi une relation théorique qui détermine les nombres de Reynolds pour divers nombres de Hartmann pour lesquels débute la paire de tourbillons stationnaires de Föppl. Le champ magnétique inhibe la formation de cette configuration.

(4) La génération de l'allée de tourbillons de Von Karman s'échappant derrière la sonde pour un nombre de Reynolds d'environ 34, produit une légère augmentation dans la loi de puissance de la formule du transfert thermique qui est encore indépendant de l'intensité du champ magnétique. Les nombres de Reynolds pour divers nombres de Hartmann pour lesquels l'échappement commence sont représentés mathématiquement. Le champ magnétique retarde l'apparition de l'allée de tourbillons et diminue sa taille.

HYDROMAGNETODYNAMISCHE WÄRMEÜBERTRAGUNG VON HEISSFILMSONDEN

Zusammenfassung—Diese Arbeit vermittelt die Ergebnisse einer experimentellen Untersuchung der hydromagnetodynamischen Wärmeübertragung von quarzbeschichteten Heissfilmsonden (0,015 cm und 0,005 cm Durchmesser), die senkrecht durch einen mit Quecksilber gefüllten Behälter bewegt werden, der axial fluchtend in einem horizontalen Magnetfeld liegt. Die Ergebnisse der Untersuchung zeigen eine Verminderung der Wärmeübertragung von der Sonde infolge des Magnetfeldes im Bereich der Reynolds-Zahlen von 0 bis 130 und im Bereich der Hartmann-Zahlen von 0 bis 4,68 für Werte des magnetischen Wechselwirkungsparameters der Grössenordnung eins. Es wurden vier Bereiche identifiziert, wovon jeder mit einer spezifischen Strömungskonfiguration um die Sonde verbunden ist. Die verschiedenen Bereiche werden wie folgt beschrieben:

1. Im Bereich der freien Konvektion unterdrückt das Magnetfeld die Wärmeübertragung durch freie Konvektion und begrenzt schliesslich die Wärmeübertragung auf die Wärmeleitung. Die Wärmeübertragung in diesem Bereich wurde durch eine Näherungslösung der Impuls- und Energiegleichung untersucht.

2. Für sehr niedrige Reynolds-Zahlen von ungefähr drei tritt eine Zunahme der Wärmübertragung gegenüber dem Zustand der freien Konvektion ein. Die Reynolds-Zahl, bei denen dieser Anfangsbereich

der erzwungenen Konvektion an Bedeutung gewinnt, ist durch ein theoretisches Kriterium vorausgesagt, das die Geschwindigkeiten der freien und erzwungenen Konvektion vergleicht. Dieses Anwachsen wird feststellbar bei niedrigen Reynolds-Zahlen in Gegenwart eines Magnetfeldes.

3. Beginnend bei einer Reynolds-Zahl von fünf, kann die Nusselt-Zahl durch ein Potenzgesetz als Beziehung der Reynolds-Zahl ausgedrückt werden, wobei die Potenz unabhängig von der Magnetfeldstärke ist. Auch eine theoretische Beziehung wird angegeben, die die Reynolds-Zahlen für verschiedene Hartmann-Zahlen bestimmt, bei denen dieses stationäre Föppl-Wirbel-Paar beginnt. Das Magnetfeld verhindert eine Formation nach diesem Modell.

4. Die Erzeugung einer Karmanschen-Wirbelablösung hinter der Sonde bei einer Reynolds-Zahl von ungefähr 34 liefert eine leichte Zunahme im Potenzgesetz der Wärmeübertragungsbeziehung, die wieder unabhängig von der Magnetfeldstärke ist. Die Reynolds-Zahlen für verschiedene Hartmann-Zahlen bei denen die Ablösung beginnt, sind mathematisch dargestellt. Das Magnetfeld verzögert den Beginn der Wirbelstrasse und unterdrückt seine Grösse.

МАГНИТОГИДРОДИНАМИЧЕСКИЙ ПЕРЕНОС ТЕПЛА ОТ НАГРЕТЫХ ПЛЕНОЧНЫХ ДАТЧИКОВ

Аннотация—В статье приводятся результаты экспериментального исследования магнитогидродинамического переноса тепла от покрытых кварцем нагретых пленочных датчиков диаметром 0,015 см и 0,005 см, перемещаемых вертикально через емкость, заполненную ртутью и установленную на одной оси с горизонтальным магнитным полем. Полученные данные свидетельствуют об уменьшении теплообмена в датчике под влиянием магнитного поля в диапазоне значений числа Рейнольдса от 0 до 130 и числа Гартмана от 0 до 4,68 при значениях параметра магнитного взаимодействия порядка единицы. Выделяются следующие четыре области теплопереноса, каждая из которых связана с особой конфигурацией течения вблизи зонда:

1. В области свободной конвекции магнитное поле подавляет свободную конвекцию, ограничивая процесс теплопроводностью. Для расчета теплообмена в этой области используется приближенное решение уравнений импульса и энергии.

2. Для очень малых значений числа Рейнольдса (порядка трех) теплоперенос возрастает по сравнению со стадией свободной конвекции. Число Рейнольдса, при котором эта начальная область вынужденной конвекции становится существенной, рассчитывается с помощью теоретического критерия, который характеризует относительные скорости свободной и вынужденной конвекции. Это возрастание теплопереноса становится заметным для малого числа Рейнольдса при наличии магнитного поля.

3. Начиная со значения числа Рейнольдса, равного примерно пяти, зависимость числа Нуссельта от числа Рейнольдса может быть выражена степенным законом с числом Рейнольдса, где показатель степени не зависит от напряженности магнитного поля. Приводится также теоретическое соотношение, определяющее значения числа Рейнольдса при различных значениях числа Гартмана, при которых возникают устойчивые парные вихри Фёкла. Магнитное поле задерживает формирование этого процесса.

4. Образование кармановской вихревой дорожки за зондом при числе Рейнольдса, равном примерно 34, приводит к небольшому увеличению показателя степени в зависимости числа Нуссельта от числа Рейнольдса, которая снова становится независимой от напряженности магнитного поля. Числа Рейнольдса для различных чисел Гартмана, при которых начинается вихреобразование, предетавлены математически. Магнитное поле задерживает образование вихревой дорожки и ограничивает ее размер.

Typographical Error Corrections to Magneto-Fluid-Mechanic Heat Transfer From Hot Film Probes

p. 1439, Nusselt definition: "K" should be "k"

p. 1444, Equation (4): "βT^2" should be "δ_T^2"

p. 1446, second column, second last line: "tbe" should be "the"

p. 1449, first column, first sentence below Fig. 9: "h" should be "n"